High resolution x-ray absorption near edge structure at the Mn K edge of manganites

2001 J. Phys.: Condens. Matter 13 3229

(http://iopscience.iop.org/0953-8984/13/14/301)

INSTITUTE OF PHYSICS PUBLISHING JOURNAL OF PHYSICS: CONDENSED MATTER

J. Phys.: Condens. Matter **13** (2001) 3229–3241 www.iop.org/Journals/cm PII: S0953-8984(01)19865-6

High resolution x-ray absorption near edge structure at the Mn K edge of manganites

Joaquín García[1], **M Concepción Sánchez, Gloria Subías and Javier Blasco**

Instituto de Ciencia de Materiales de Aragón and Departamento de Física de la Materia Condensada, Consejo Superior de Investigaciones Científicas y Universidad de Zaragoza, 50009 Zaragoza, Spain

E-mail: jgr@posta.unizar.es

Received 7 December 2000, in final form 19 February 2001

Abstract

We report a systematic study of manganese perovskites, $RE_{1-x}D_xMnO_3$ (RE = rare earth; D = Ca, Sr), by means of x-ray absorption near edge structure (XANES) spectroscopy at the Mn K edge. High resolution has been achieved by recording the intensity of the Mn Kβ fluorescence spectrum. All the samples show a unique resonance at the Mn K edge. This common feature does not depend on small changes in the local structure around the Mn atom. The XANES spectra of mixed ($0 < x < 1$) composition compounds cannot be obtained by linear combination of $REMnO_3$ and $DMnO_3$ spectra. Therefore, Mn^{3+} and Mn^{4+} ions cannot be distinguished in intermediate $RE_{1-x}D_xMnO_3$ compounds, either spatially or temporally. The possibility of a charge disproportionation is also considered and discussed in the paper.

1. Introduction

The recent extensive study of the colossal magnetoresistance (CMR) phenomena in perovskite-type manganites has shown exotic properties of these mixed valence compounds. The phenomenology shown by the perovskites $RE_{1-x}D_xMnO_3$ (RE = rare earth atom, D = divalent atom such as Ca, Sr) is very rich; it depends on the RE^{3+}/D^{2+} content ratio, RE^{3+}/D^{2+} average ionic size and RE^{3+}/D^{2+} size mismatch [1]. In the archetypal $La_{1-x}Ca_xMnO_3$ series, a metal–insulator transition coupled to a ferromagnetic ordering has been found for $0.2 \leqslant x \leqslant 0.5$ showing giant magnetoresistance. This behaviour was roughly explained by the double exchange interaction [2–4]. Different kinds of electronic localization and spin ordering phenomena have been observed for $x < 0.2$ and $x \geqslant 0.5$, including the so-called 'charge-ordered state' [5]. The magnetic ground state for the latter composition range is antiferromagnetic but different types of magnetic structure are found depending on

[1] Corresponding author: Joaquin García Ruiz, ICMA—Departamento de Física de la Materia Condensada, CSIC—Universidad de Zaragoza, 50009 Zaragoza, Spain.

0953-8984/01/143229+13$30.00

the x value. The substitution of La by other RE with smaller ion size reduces the strength of the ferromagnetic interactions and expands the composition range for the charge-ordered structures [1]. In some compounds, transitions between the insulating charge-ordered state and the metallic ferromagnetic state can be achieved by applying an external magnetic field, an electrical field or x-ray radiation [6]. Recently, the finding of different ferrimagnetic or metallic antiferromagnetic states has expanded the phenomenology observed in these compounds [7].

The problem of the electronic localization in manganites is still a matter of discussion in spite of the large amount of work done. One of the main goals of our research is the identification of the electronic state for the Mn atom in perovskites compounds. Usually, mixed valence manganites have been described considering an ionic model, i.e. as $RE_{1-x}D_xMn^{3+}_{1-x}Mn^{4+}_xO_3$. In this way, it is thought that charge-ordering states arise from the localization of e_g electrons on Mn^{3+} ions and that these ions are periodically ordered in the lattice to minimize the Coulomb repulsion. However, the e_g electrons are delocalized on the Mn atoms in the metallic ferromagnetic phase and thermal activated hopping between adjacent Mn atoms is proposed for the semiconducting paramagnetic phase. The giant magnetoresistance in charge-ordered systems has been explained in terms of melting of the charge ordering by an external magnetic field [8].

The valence state of the manganese atoms in mixed valence perovskites has been the subject of several works but the reported results show discrepancy and seem to depend on the experimental techniques used. Thermoelectric power experiments indicate a number of charge carriers, of hole-like type, higher than those expected from the doping ratio [9]. The authors suggest a disproportionation of the Mn^{3+} states into Mn^{4+} and Mn^{2+} states. On the other hand, electronic paramagnetic resonance measurements show the absence of isolated Mn ions in 2+, 3+ or 4+ states at room temperature [10]. XPES and oxygen K edge x-ray absorption spectroscopies seem to indicate that spectra of doped samples can be obtained by linear combination of the end members of the series. However, there is a significant discrepancy between the weighted and the experimental spectrum [11]. In summary, the support of spectroscopic techniques for a full charge segregation model does not seem to be very convincing.

We have analysed the valence state of the Mn atoms by using the Mn K edge x-ray absorption spectra in a previous publication [12]. Our attention was mainly focused on magnetoresistive samples showing a transition between semiconducting paramagnetic and metallic ferromagnetic states, i.e. $RE_{1-x}D_xMnO_3$ compounds with $x \approx 0.33$. Our results showed that Mn does not fluctuate between 3+ and 4+ states and, therefore, an ionic approximation is not valid for these compounds. Accordingly, we found a unique magnetic signature for Mn using x-ray magnetic circular dichroism measurements [12]. Similar results were obtained by other x-ray absorption experiments [13–16]. Recent x-ray anomalous diffraction studies [17–19], claim for the observation of charge ordering in manganites with $x = 0.5$.

The aim of this work is to determine whether the mixed valence manganites can be described or not as an inhomogeneous mixture of Mn^{3+} and Mn^{4+} ionic states. This study has not only focused on magnetoresistive samples but also on insulating ones, some of them with the so-called charge ordering state.

We present XANES spectra at the manganese K edge of $RE_{1-x}Ca_xMnO_3$ (RE = La, Tb, $x = 1, 1/3, 1/2, 2/3$ and 0), $RE_{0.5}D_{0.5}MnO_3$ (RE = La, Tb, D = Sr, Ca) and $La_{0.5}Sr_{1.5}MnO_4$ samples by measuring both the total fluorescence yield intensity and the Mn Kβ fluorescence intensity (Hastings' method) [20]. This method improves the resolution beyond the broadening produced by the core-hole lifetime. Transmission experiments on the charge-ordered materials through the phase transition have been also analysed. Our results for these compounds indicate that the electronic state of manganese atoms cannot be described by a weighted addition of typical Mn^{3+} and Mn^{4+} spectra.

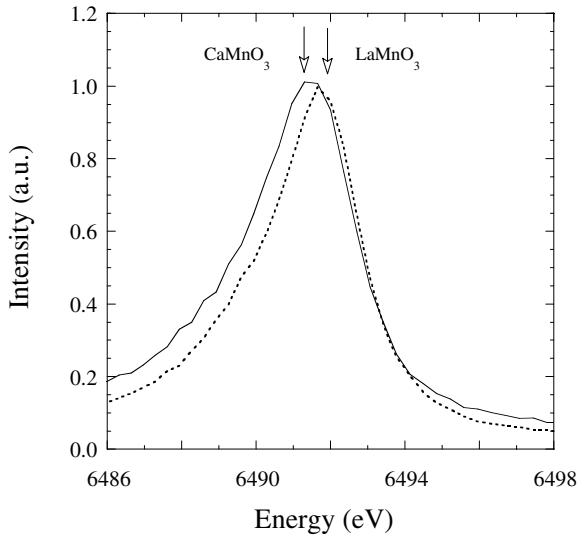

Figure 1. Kβ emission fluorescence spectra of $CaMnO_3$ (continuous line) and $LaMnO_3$ (dotted line). The energy at which the intensity of the Mn Kβ emission has been recorded is indicated by arrows.

2. Experimental details

The preparation of the different samples were carried out by standard ceramic procedures or using a sol–gel method by the citrate route. The procedures are described elsewhere [21]. The samples were characterized by means of x-ray powder diffraction as single-phase materials. Oxygen content was tested by titration redox using $KMnO_4$ and Mohr's salt. Magnetic and electrical transport characterization were also carried out and the macroscopic properties of our samples are in agreement with those reported elsewhere [1, 21]. The experiments were performed at the beam-line ID26 of the ESRF in Grenoble. A Si(311) monochromator was used and the total current of the storage ring was about 200 mA. XANES spectra at the Mn K edge were recorded by measuring the total fluorescence yield (TFY) and by analyzing the Kβ fluorescence line by means of a Rowland circle spectrometer based on a spherical bent Si(440) monochromator. The resolution was about 0.5 eV. Kβ emission and total fluorescence spectra have been recorded simultaneously.

The intensity of the Kβ fluorescence line has been measured at the emission spectrum peak as shown in figure 1. Emission fluorescence spectra are similar to those reported by Tyson *et al* [16] and we also note that the emission peak for $CaMnO_3$ is broader than the one for $LaMnO_3$. Moreover, there is a shift to higher energies for the latter.

XANES spectra of $Tb_{0.5}Ca_{0.5}MnO_3$ and $La_{0.5}Ca_{0.5}MnO_3$ at different temperatures have been measured at the beamline BM29 of the ESRF in Grenoble in transmission mode, using a Si(311) monochromator.

3. Results

Normalized XANES spectra for $La_{1-x}Ca_xMnO_3$ and $Tb_{1-x}Ca_xMnO_3$ compounds at room temperature obtained by measuring both TFY and Mn Kβ line fluorescence are compared in figure 2. Different physical features are clearly resolved better by measuring the Mn Kβ line

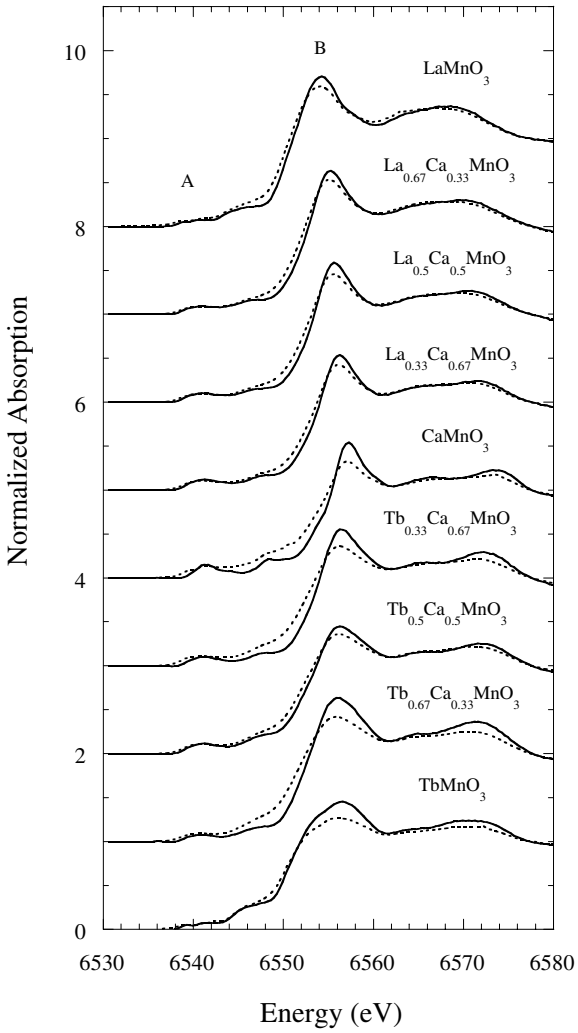

Figure 2. Normalized XANES spectra of $La_{1-x}Ca_xMnO_3$ and $Tb_{1-x}Ca_xMnO_3$ series at room temperature recorded by Mn Kβ emission (continuous line) and total fluorescence yield (dashed line).

intensity than in the conventional fluorescence spectra. As we have mentioned, the spectra were measured at the peak of the emission line, as Tanaka *et al* [22] suggest, to be regarded as the absorption spectrum with a smaller width. Moreover, the Mn Kβ fluorescence spectra could be sensitive to the spin state [23], so we have checked the equivalence between both kinds of measurement. We noted that the conventional TFY spectra can be obtained from the Kβ spectra by a convolution with a Lorentzian function of about 0.8 eV width. The agreement between the convoluted and the total fluorescence spectra is good. The main difference is restricted to a feature in the $CaMnO_3$ spectrum (A_1 pre-peak of figure 6, discussed below). In this case, the sensitivity of the Kβ fluorescence to the spin could be responsible for the discrepancy. All the other features of the $CaMnO_3$ spectrum and of the other spectra are present in the two modes of recording.

The spectral line shapes are similar for all samples. They are composed by a pre-edge structure (denoted as A in figure 2) and a main resonance at the edge, characteristic of the Mn octahedral coordination (denoted as B in figure 2). The first pre-edge peak is located at about 10 eV below the inflection point of the edge and its intensity grows significantly with increasing Ca content of the sample, i.e. with increasing content of formal Mn^{4+}. The main difference among the spectra arises from the chemical shift. This is taken from the first inflection point of the absorption edge and it shifts to higher energies as the formal Mn^{4+} content increases. The shift is nearly linear with the formal Mn valence state and it reaches a value of about 4.5 eV between $REMnO_3$ and $CaMnO_3$ [12, 13]. The spectral differences beyond the absorption edge are due to small changes in the local structure among the samples and can be explained in terms of multiple scattering processes of the outgoing photoelectron.

3.1. Main edge

One of the main points to be solved is to determine whether the spectra of $RE_{1-x}Ca_xMnO_3$ samples can be described as a bimodal distribution of Mn^{3+} and Mn^{4+} ions. For this purpose we used for the Mn^{3+} spectrum that of $REMnO_3$ and for Mn^{4+} that of $CaMnO_3$. Furthermore, we have tried to reproduce the XANES spectra of doped compounds by the weighted sum of the end-member spectra, i.e. $(1-x)\,REMnO_3+xCaMnO_3$. The comparisons between the weighted and the experimental high-resolution spectra are shown in figure 3. Although the edge position is reasonably well reproduced, strong differences between calculated and experimental spectra are obtained for all the samples. In particular, the slope of the experimental edge is sharper and the two main structures displayed in the calculated spectra are absent in the experimental ones. This agrees with the fact that the spectrum of a photoabsorbing atom in a single electronic state shows a unique resonance and sharper absorption edge than the one associated with the mixture of two atoms with different electronic or valence states.

It is well known that the shape of the XANES spectrum also depends on the particular local structure of the photoabsorbing atom. Consequently, it can be argued that the above analysis could be non-conclusive. In order to extract the common experimental features for all the samples, independently of small variations in the local structure, we have also measured the XANES spectra of different $RE_{0.5}Ca(Sr)_{0.5}MnO_3$ samples and of the $La_{0.5}Sr_{1.5}MnO_4$ compound. Our aim was to check how the XANES spectrum is affected by small changes in the local structure. In this way, we studied samples with different rare earth or divalent atoms keeping unchanged the ratio $Mn^{3+}/Mn^{4+} = 1$. The results for several compounds are shown in figure 4. We observe similar spectra for all the samples. They exhibit a main resonance with a similar slope at the edge. There are small variations in the intensity of the peak at the main resonance but the width is nearly equal for all of them. This is true even for $La_{0.5}Sr_{1.5}MnO_4$ which has a different crystallographic structure. The main difference among the spectra, arising from the local structure, is located at energies above the main resonance. Therefore, the presence of the main peak (denoted as B in figure 2) is common for all these manganites and it can be used as a mark of the Mn electronic state. Consequently, one can say that the differences obtained for the main edge resonance between the calculated and the experimental spectra in figure 3 cannot be attributed to the different local structure. Instead, it is clear that the valence state of the Mn atom for intermediate concentrations cannot be described as a mixture of the two valence states (3+ and 4+) associated to the end members of the series.

3.2. Pre-edge region

Figure 5 shows the pre-edge region of the XANES spectra for the $La_{1-x}Ca_xMnO_3$ series; they were measured by recording the intensity of the Kβ emission. A main difference is observed

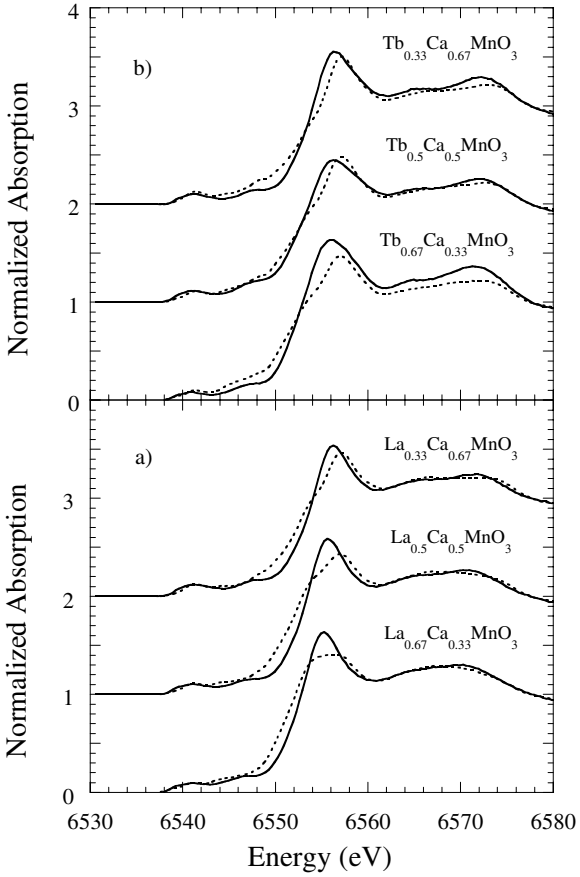

Figure 3. Comparison between the normalized high-resolution XANES spectra of $La_{1-x}Ca_xMnO_3$ (panel a) and $Tb_{1-x}Ca_xMnO_3$ (panel b) series (continuous line) and the spectra obtained by the weighted addition of the end-member compound spectra (dashed line).

between undoped ($LaMnO_3$ and $CaMnO_3$) and doped compounds: the resonance A is clearly split for the undoped compounds (hereafter denoted as A_1 and A_2) while this splitting is less apparent for the doped compounds. Similar results have been obtained for the $Tb_{1-x}Ca_xMnO_3$ samples. The pre-edge region cannot be obtained as a weighted sum of the spectra of the parent compounds. Moreover, the pre-peak structures of the TFY spectra can be well reproduced by convolution of the Kβ spectra except for the A_1 peak which is absent in the Kβ spectrum of $CaMnO_3$ as is shown in figure 6. The lack of the first state (A_1) in the Kβ emission spectra indicates the majority spin character for this peak, i.e. this transition occurs mainly to states with spin parallel to the Mn 3d spin [23]. Consequently, the A_1 state of $LaMnO_3$ and of the doped samples does not seem to be sensitive to the spin. The splitting between A_1 and A_2 is 1.7 eV and 2.0 eV for $LaMnO_3$ and $CaMnO_3$ respectively. This splitting is around 1.3 eV for doped samples. Moreover, we note that the peak A_2 continuously shifts to higher energies as the average valence state of Mn atoms increases. The intensity of the pre-peaks increases with increasing Ca content. This result suggests an increase of the covalence between Mn 3d and O p empty states. It is noteworthy that the spectra of the mixed valence compounds are very similar to each other, but quite different from the ones of the end-member samples. The pre-edge

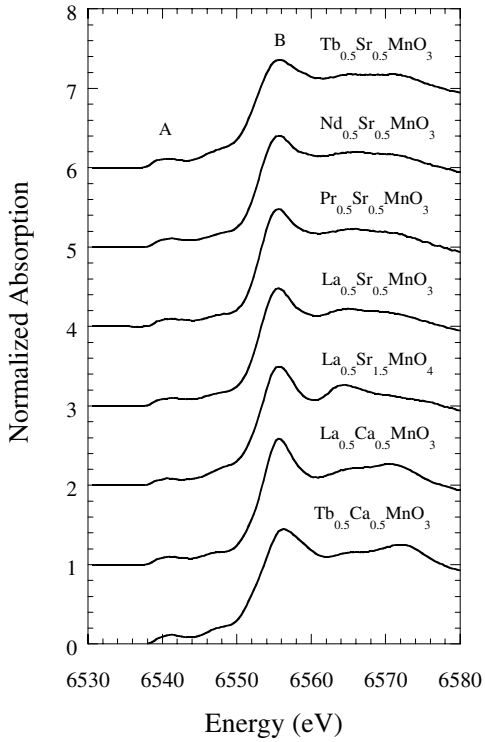

Figure 4. Normalized XANES spectra recorded by Mn Kβ emission of $RE_{0.5}Sr_{0.5}MnO_3$, $RE_{0.5}Ca_{0.5}MnO_3$ and $La_{0.5}Sr_{1.5}MnO_4$ compounds.

spectra for samples with $Mn^{4+}/Mn^{3+} = 1$ (not reported previously) are also almost identical. Therefore, the assumption of electronic transitions to the same band states for both the mixed valence and the undoped compounds is difficult to reconcile with the experimental data.

The pre-peaks of the XANES spectra have usually been assigned to transitions to the Mn 3d empty states. These transitions are forbidden by the dipolar selection rule and they become allowed if the 3d states hybridize with the p states of neighbouring atoms. It is thought that this hybridization is mainly with oxygen 2p-states. A recent work by Elfimov *et al* shows that a strong hybridization of Mn d states with 4p states of adjacent Mn atoms through the oxygen occurs in $LaMnO_3$ [24]. A similar interpretation has been given by Joly *et al* to describe the pre-peaks in TiO_2 [25]. In summary, it seems that the pre-edge features give valuable information on the splitting of the empty Mn d band and on the hybridization with the surrounding atoms. Recently, Bridges *et al* [26] assigned the A_1 peak to the majority e_g band and the A_2 peak to the minority e_g and t_{2g} bands. The comparison between conventional and Kβ spectra (see figure 6) shows that the assignation of A_1 peak to the majority e_g band is justified for $CaMnO_3$, but not for the rest of the samples. The point we would like to emphasize is that the spectra of the parent compounds are very different from the mixed valence ones, indicating that a particular state is chosen when the valence is integer.

3.3. Thermal evolution of XANES spectra of $La_{0.5}Ca_{0.5}MnO_3$ and $Tb_{0.5}Ca_{0.5}MnO_3$

We have studied the thermal evolution of the XANES spectra for the magnetoresistive $x = 0.33$ compound in the past [12]. No significant changes were noticed in the phase transition between

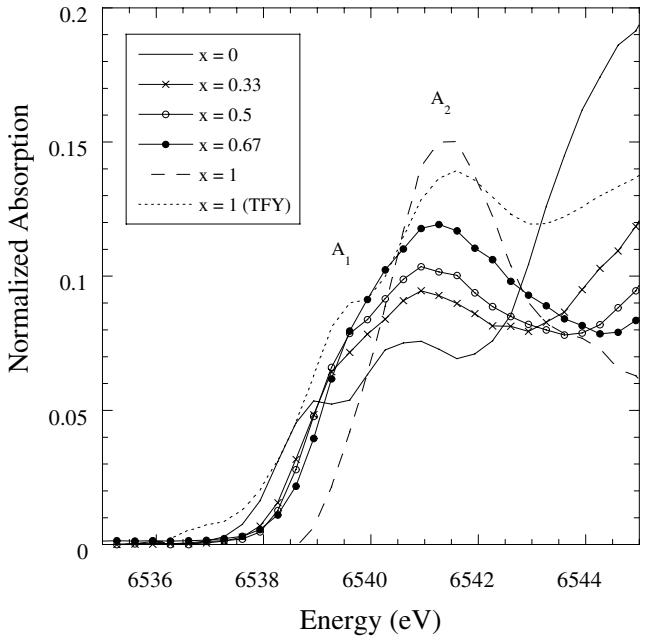

Figure 5. Pre-edge region of the high-resolution XANES spectra of the $La_{1-x}Ca_xMnO_3$ series. Total fluorescence yield (TFY) of $CaMnO_3$ (continuous line) is also reported.

the semiconducting paramagnetic and the metallic ferromagnetic phases. Accordingly, we concluded that the variations in the electronic state of Mn ions across this transition are small. We have enlarged this study by analyzing charge-ordered compounds. The comparison of the XANES spectra of $La_{0.5}Ca_{0.5}MnO_3$ and $Tb_{0.5}Ca_{0.5}MnO_3$ at different temperatures is shown in figure 7. $La_{0.5}Ca_{0.5}MnO_3$ shows two phase transitions with decreasing temperature [27]: a first one from the paramagnetic semiconducting phase to a ferromagnetic metallic one at around 230 K (similar to the $x = 0.33$ sample) and another one at 150 K from the ferromagnetic metallic to an insulating charge-ordered phase. The latter transition is coupled to an antiferromagnetic ordering in this case. On the other hand, $Tb_{0.5}Ca_{0.5}MnO_3$ shows a phase transition from a semiconducting–paramagnetic phase to an insulator charge-ordered phase at 300 K. For this compound, this transition is not coupled to the antiferromagnetic ordering which appears at 140 K [28]. The plots of figure 8 show identical features at all temperatures for each sample. In order to distinguish variations at different temperatures, the XANES spectra have been subtracted as shown in figure 8. The main differences are at the absorption edge and main resonance, being larger for the $Tb_{0.5}Ca_{0.5}MnO_3$ (lower than 8%) than for $La_{0.5}Ca_{0.5}MnO_3$ (lower than 2%). The differences cannot be directly related to the derivative spectra, which guarantees good energy reproducibility. The observed differences are very small and they seem to be related to small structural change across the different phase transitions. The differences at the edge are larger for Tb manganites than for La ones: this fact can be ascribed to the structural distortion of the charge-ordering phase, larger in $Tb_{0.5}Ca_{0.5}MnO_3$. The change in the XANES spectrum at the charge-ordering phase transition is opposite to the one found for magnetoresistive manganites at the metal–insulator phase transition [12, 26]. Therefore, the local structure of Mn atoms in the metallic state is more homogeneous or symmetric than in the other two phases. The pre-edge structures also change

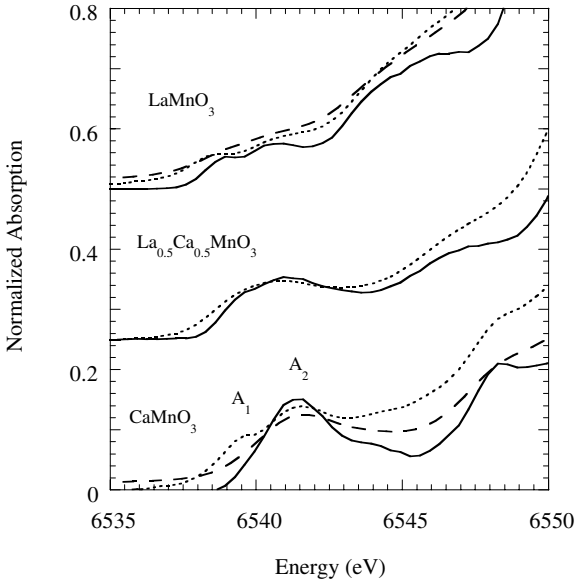

Figure 6. Comparison of the pre-edge XANES region of high-resolution spectra (continuous line) with the total fluorescence yields spectra (dotted line) for $LaMnO_3$, $La_{0.5}Ca_{0.5}MnO_3$ and $CaMnO_3$. Broken lines are obtained by convolution of TYF spectra. The agreement between broken and dotted lines is fair for $LaMnO_3$ but fails to reproduce the A_1 peak for $CaMnO_3$ spectra.

at the charge-ordering phase transition and, again, the behaviour is opposite to that observed in the metal–insulator transition for the magnetoresistive samples. The comparison of this feature among the charge-ordered phase, the paramagnetic phase and the metallic phase indicates an increase of the p–d hybridization for the latter phase. This result would nicely be correlated with the different electrical behaviour of these phases. In any case, the changes in both electronic state and local structure around the Mn atom are very small among these phases.

4. Discussion

We have shown that spectra of $RE_{1-x}Ca_xMnO_3$ samples cannot be obtained by the weighted addition of the spectra of the end-members of the series. However, it does not mean that all the Mn atoms would be identical from a local geometrical and electronic point of view. In order to check the sensitivity of our data to small differences between Mn atoms, we have also compared the experimental spectra of $La_{1/2}Ca_{1/2}MnO_3$ with the weighted sum of $La_{2/3}Ca_{1/3}MnO_3$ and $La_{1/3}Ca_{2/3}MnO_3$ spectra. The results are displayed in figure 8 where calculated and experimental spectra are alike; similar results have been obtained for $Tb_{1/2}Ca_{1/2}MnO_3$. One can infer from this comparison that both electronic state and local structure of Mn atoms are very similar for doped $RE_{1-x}Ca_xMnO_3$ samples with values of x not far from each other. This is true even for samples whose macroscopic behaviour is completely different (we note that $Tb_{1/2}Ca_{1/2}MnO_3$ shows a charge-ordered state at room temperature but not $Tb_{2/3}Ca_{1/3}MnO_3$ or $Tb_{1/3}Ca_{2/3}MnO_3$). Furthermore, a limit to the accuracy of the XANES technique can be established. From the analysis of the XANES spectra, one can affirm that neither Mn^{3+} nor Mn^{4+} exist in the intermediate $RE_{1-x}Ca_xMnO_3$ compounds. Therefore, the XANES study shows that a description in terms of intermediate valence should be more appropriate to describe this system. The similitude between calculated and experimental spectra in figure 8 shows that

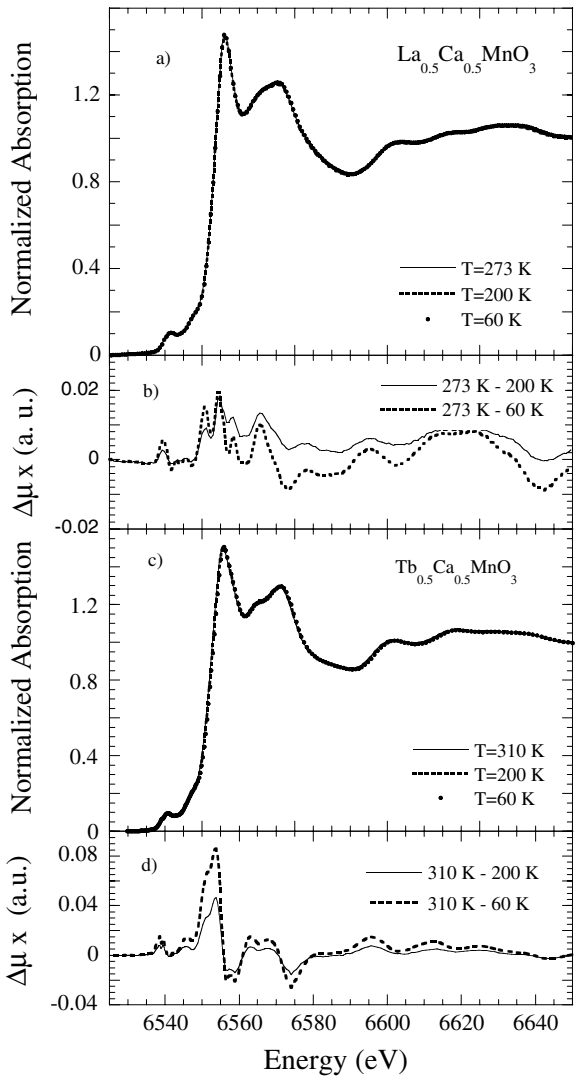

Figure 7. XANES transmission spectra of $La_{0.5}Ca_{0.5}MnO_3$ (panel a) and $Tb_{0.5}Ca_{0.5}MnO_3$ (panel c) at temperatures above and below the charge ordering phase transition. Differences between high and low temperature spectra are also shown.

the existence of Mn atoms with different electronic charge densities ranging from $Mn^{3.33+}$ to $Mn^{3.67+}$ in the $RE_{1/2}Ca_{1/2}MnO_3$ sample cannot be discarded.

Much experimental evidence against the presence of two ionic states—Mn^{3+} and Mn^{4+}– in mixed valence manganites is emerging nowadays. First of all, our experimental results concur with those obtained by using x-ray spectroscopies [11–16]. Park *et al* [11] were able to calculate both the Mn 2p x-ray photoelectron and the O 1s absorption spectra of intermediate compositions, by linear combination of the end-member spectra. However, a large discrepancy between calculated and experimental spectra is observed in agreement with our results. Tyson *et al* [16] managed to reproduce the Mn Kβ emission spectra of intermediate concentrations by combining the end-member spectra but again, a more complex doping effect

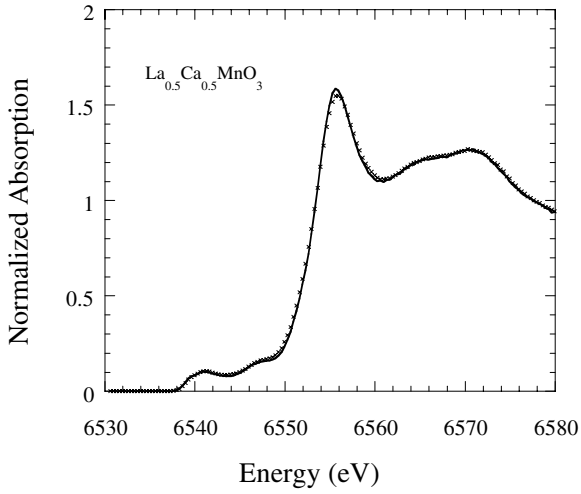

Figure 8. XANES spectra in the high-resolution mode of $La_{0.5}Ca_{0.5}MnO_3$ (line) compared with the addition of 0.5 $La_{0.33}Ca_{0.66}MnO_3$ + 0.5$La_{0.66}Ca_{0.33}MnO_3$ (crosses).

seems to exist because of lack of a linear relationship between the weighting factor and the stoichiometric composition for the whole series. In addition, other techniques such as EPR [10] and thermoelectric power results are also in controversy with the simple ionic model [9].

In summary, all of these works are indicating that the pure ionic model is a rough approximation for the electronic properties of mixed valence manganites. This ionic model has been widely used in the study of the charge ordering states in manganites, so we focus our discussion on this kind of compound in order to address our experimental results with the findings of other techniques. The charge-ordered states are concluded from transmission electron microscopy [29] and from both x-ray [28] and neutron diffraction experiments [27]. These papers report changes in the lattice parameters and the appearance of superstructure diffraction peaks. The Rietveld refinement of the charge-ordered phases has shown the presence of two kinds of MnO_6 octahedron ascribed to Mn^{3+} and Mn^{4+} ions. However, the lack of sensitivity of these techniques does not permit us to differentiate changes in the Mn electronic structure. A powerful method to improve the resolution of diffraction techniques is the use of resonant scattering at the Mn K edge. Recent resonant scattering experiments at the Mn K edge on $La_{0.5}Sr_{1.5}MnO_4$, $Pr_{0.5}Ca_{0.5}MnO_3$ and $Nd_{0.5}Sr_{0.5}MnO_3$ have been reported [17–19] and the authors claim a real charge ordering in these samples. We note that the same charge-ordering model is used for the three materials although a different azimuthal behaviour is reported for the intensity of the resonant reflections. We have reanalysed these data and they will be published separately [30]. Our analysis shows that no real charge ordering of Mn^{3+} and Mn^{4+} exists in these compounds: instead these experiments demonstrate the existence of two kinds of Mn atom with two different geometrical environments. Furthermore, the inadequacy of the ionic model seems to be general for mixed valence oxides, especially for transition metals in a high oxidation state. Recent resonant scattering experiments in magnetite, which is the archetype model for charge-ordering systems, have shown that the differentiation between octahedral Fe^{3+} and Fe^{2+} ions has no sense in this system [31].

There are also theoretical papers pointing out the insufficiency of a charge-ordering model to describe these compounds. Recent calculations made by Anisimov *et al* for the electronic structure for $Pr_{0.5}Ca_{0.5}MnO_3$ have found two types of Mn e_g configuration with almost identical

charge densities [32]. Moreover, a theoretical model to explain the lack of resonant scattering associated to the charge ordering in $La_{1/8}Sr_{7/8}MnO_3$ concludes that the formal Mn^{4+} atom would have an electronic occupancy close to $3d^4$ [33]. One can deduce from these studies that the differentiation between Mn^{3+} or Mn^{4+} is only formal and it is only made on the basis of the different symmetry of the e_g states which mix to form the 3d band. Mizokawa and Fujimori also obtained similar conclusions in their calculations [34].

Bearing in mind these results, the electronic localization in manganites (either in the paramagnetic phase or in the charge-ordered phase) is now an open question. Our experiments show the lack of charge localization on individual atoms. Therefore, the electronic localization must be extended over several Mn atoms. A cluster localization giving rise to local phase segregation [35], or to molecular polarons or to the presence of the conducting states with lower dimensionality, as it was shown for the $Nd_{0.45}Sr_{0.55}MnO_3$ compound [7], would explain the electrical transport behaviour.

5. Conclusions

The electronic state of Mn atoms in mixed valence manganites has been studied by means of x-ray absorption spectroscopy at the Mn K edge. Higher resolution than in conventional measurements has been achieved by measuring the Mn Kβ fluorescence line.

We have found a unique resonance at the edge in the XANES spectra of intermediate composition $RE_{1-x}Ca_xMnO_3$ samples. The features of these XANES spectra do not depend on small changes in the local structure around the Mn atom. However, the spectra of the intermediate composition samples cannot be reproduced by a linear combination of $REMnO_3$ and $CaMnO_3$ spectra. Accordingly, the electronic state of Mn atoms in these compounds cannot be considered as a mixture of Mn^{3+} and Mn^{4+} pure states. Furthermore, the strong similitude of XANES spectra for intermediate doping compounds does not discard the presence of a charge disproportionation. A charge disproportionation provides a suitable explanation for both the macroscopic properties of these compounds and the lack of significant changes in the XANES spectra through different phase transitions occurring in these samples. Moreover, the pre-edge features indicate well defined but different electronic states for the end-member of the series ($REMnO_3$ and $CaMnO_3$) while the mixed valence compounds show a large similitude among them in their electronic states. Furthermore, our results suggest minor changes in both electronic configuration and local environment of Mn ions, by varying the temperature.

In conclusion, an ionic model is a very rough approximation to describe the electronic properties of manganites and further models, such as molecular localization or the formation of charge density waves, must be tested to account for the electronic localization observed in the so-called charge-ordered compounds.

Acknowledgments

We would like to thank ESRF for beam time granting, Dr C Gauthier, Dr A Solé and Dr M H Krisch for their kind assistance in the experiment. This work has been supported by the Spanish CICYT project no MAT99-0847.

References

[1] Coey J M D, Viret M and Von Molnar S 1999 *Adv. Phys.* **48** 167
[2] Zener C 1955 *Phys. Rev.* B **82** 403
[3] Ibarra M R, Algarabel P A, Marquina C, Blasco J and García J 1995 *Phys. Rev. Lett.* **75** 3541

[4] Millis A J, Littlewood P B and Shraiman B I 1995 *Phys. Rev. Lett.* **74** 5144
[5] Chen C H, Cheong S-W and Cooper A S 1993 *Phys. Rev. Lett.* **71** 2461
Kuwahara H, Tomioka Y, Asamitsu A, Morimoto Y and Tokura Y 1995 *Science* **270** 961
[6] Tomioka Y, Asamitsu A, Moritomo Y and Tokura Y 1995 *J. Phys. Soc. Japan* **64** 3626
Asamiysu A, Tomioka Y, Kuwahara H and Tokura Y 1997 *Nature* **388** 59
Kiryukhin V, Casa D, Hill J P, Keimer B, Vigilante A, Tomioka Y and Tokura Y 1997 *Nature* **386** 813
[7] Kuwahara H, Okuda T, Tomioka Y, Asamitsu A and Tokura Y 1999 *Phys. Rev. Lett.* **82** 4316
[8] Kusters R M, Singleton J, Keen D A, McGreevy R and Hayes W 1989 *Physica* B **155** 362
Urushibara A, Moritomo Y, Arima T, Asamitsu A, Kido G and Tokura Y 1995 *Phys. Rev.* B **51** 14 103
[9] Hundley M F and Neumeier J J 1997 *Phys. Rev.* B **55** 11 511
[10] Oseroff S B, Torikachvili M, Singley J, Ali S, Cheong S-W and Schultz S 1996 *Phys. Rev.* B **53** 6521
[11] Park J H, Chen C T, Cheong S-W, Bao W, Meigs G, Chakairan V and Idzerda Y U 1996 *Phys. Rev. Lett.* **76** 4215
[12] Subías G, García J, Proietti M G and Blasco J 1997 *Phys. Rev.* B **56** 8183
[13] Booth C H *et al* 1998 *Phys. Rev.* B **57** 10 440
Croft M, Sillis D, Greenblatt M, Lee C, Cheong S-W, Ramanujachary K V and Tran D 1997 *Phys. Rev.* B **55** 8726
[14] Liu R S, Wu J B, Chang C Y, Lin J G, Huang C Y, Chen J M and Liu R G 1996 *J. Solid State Chem.* **125** 112
[15] Pellegrin E, Tjeng L H, de Groot F M F, Hesper R, Sawatzky G A, Moritomo Y and Tokura Y 1997 *J. Electron Spectrosc. Relat. Phenom.* **86** 115
[16] Tyson T A, Qian Q, Kao C C, Rueff J P, de Groot F M F, Croft M, Cheong S-W, Greenblatt M and Subramanian M A 1999 *Phys. Rev.* B **60** 4665
[17] Murakami Y, Kawada H, Kawada H, Tanaka M, Arima T, Moritomo Y and Tokura Y 1998 *Phys. Rev. Lett.* **80** 1932
[18] Nakamura K, Arima T, Nakazawa A, Wakabayashi Y and Murakami Y 1999 *Phys. Rev.* B **60** 2425
[19] Vonzimmerman M, Hill J P, Gibbs D, Blume M, Casa D, Keimer B, Murakami Y, Tomioka Y and Tokura Y 1999 *Phys. Rev. Lett.* **83** 4872
[20] Hämäläinen K, Siddons D P, Hastings J B and Berman L E 1991 *Phys. Rev. Lett.* **67** 2850
[21] Blasco J, Ritter C, García J, de Teresa J M, Pérez-Cacho J and Ibarra M R 2000 *Phys. Rev.* B **69** 5609
Ibarra M R, de Teresa J M, Blasco J, Algarabel P A, Marquina C, García J, Stankiewitz J and Ritter C 1997 *Phys. Rev.* B **56** 8252
de Teresa J M *et al* 1996 *Phys. Rev.* B **54** 1187
[22] Tanaka S, Okada K and Kotani A 1994 *J. Phys. Soc. Japan* **63** 2780
[23] Hämäläinen K, Kao C C, Hastings J B, Siddons D P, Berman L E, Stojanoff V and Cramer S P 1992 *Phys. Rev.* B **46** 14 274
[24] Elfimov I S, Anisimov V I and Sawatzky G A 1999 *Phys. Rev. Lett.* **82** 4264
[25] Joly Y, Cabaret D, Renevier H and Natoli C R 1999 *Phys. Rev. Lett.* **82** 2398
[26] Bridges F, Booth C H, Kwei G H, Neumeier J J and Sawatzky G A 2000 *Phys. Rev.* B **61** R9237
[27] Radaelli P G, Marezio M, Hwang H Y, Cheong S-W and Batlogg B 1995 *Phys. Rev. Lett.* **75** 4488
Radelli P G, Cox D E, Marezio M and Cheong S-W 1997 *Phys. Rev.* B **55** 3015
[28] Blasco J, Garcia J, de Teresa J M, Ibarra M R, Perez J, Algarabel P A, Marquina C and Ritter C 1997 *J. Phys.: Condens. Matter* **9** 10 321
[29] Chen C H, Cheong S-W and Hwang H Y 1997 *J. Appl. Phys.* **81** 4326
[30] García J, Sanchez M C, Blasco J, Subías G and Proietti M G 2001 *J. Phys.: Condens. Matter* **13**
[31] García J, Subías G, Proietti M G, Renevier H, Joly Y, Hodeau J L, Blasco J, Sanchez M C and Berar J F 2000 *Phys. Rev. Lett.* **85** 578
[32] Anisimov V L, Korotin M A and Terakura K 1997 *Phys. Rev.* B **55** 15 494
[33] Mizokawa T, Khomskii D I and Sawatzky G A 2000 *Phys. Rev.* B **61** R3776
[34] Mizokawa T and Fujimori A 1997 *Phys. Rev.* B **56** R493
[35] de Teresa J M, Ibarra M R, Algarabel P A, Ritter C, Marquina C, Blasco J, García J, Del Moral A and Arnold Z 1997 *Nature* **386** 256